Brain Proteomics Supports the Role of Glutamate Metabolism and Suggests Other Metabolic Alterations in Protein L-Isoaspartyl Methyltransferase (PIMT)-Knockout Mice

Hongqian Yang,[†] Jonathan D. Lowenson,[‡] Steven Clarke,[‡] and Roman A. Zubarev*,[†,§]

[†]Division of Physiological Chemistry I, Department of Medical Biochemistry and Biophysics, Karolinska Institutet, Scheeles väg 2, SE-17 177 Stockholm, Sweden

[‡]Department of Chemistry and Biochemistry and the Molecular Biology Institute, University of California, Los Angeles, California 90095, United States

[§]SciLifeLab, Stockholm, Sweden

S *Supporting Information*

ABSTRACT: Protein L-isoaspartyl methyltransferase (PIMT) repairs the isoaspartyl residues (isoAsp) that originate from asparagine deamidation and aspartic acid (Asp) isomerization to Asp residues. Deletion of the gene encoding PIMT in mice (*Pcmt1*) leads to isoAsp accumulation in all tissues measured, especially in the brain. These PIMT-knockout (PIMT-KO) mice have perturbed glutamate metabolism and die prematurely of epileptic seizures. To elucidate the role of PIMT further, brain proteomes of PIMT-KO mice and controls were analyzed. The isoAsp levels from two of the detected 67 isoAsp sites (residue 98 from calmodulin and 68 from glyceraldehyde-3-phosphate dehydrogenase) were quantified and found to be significantly increased in PIMT-KO mice ($p < 0.01$).

Additionally, the abundance of at least 151 out of the 1017 quantified proteins was found to be altered in PIMT-KO mouse brains. Gene ontology analysis revealed that many down-regulated proteins are involved in cellular amino acid biosynthesis. For example, the serine synthesis pathway was suppressed, possibly leading to reduced serine production in PIMT-KO mice. Additionally, the abundances of enzymes in the glutamate–glutamine cycle were altered toward the accumulation of glutamate. These findings support the involvement of PIMT in glutamate metabolism and suggest that the absence of PIMT also affects other processes involving amino acid synthesis and metabolism.

KEYWORDS: *proteomics, tandem mass spectrometry, posttranslational modifications*
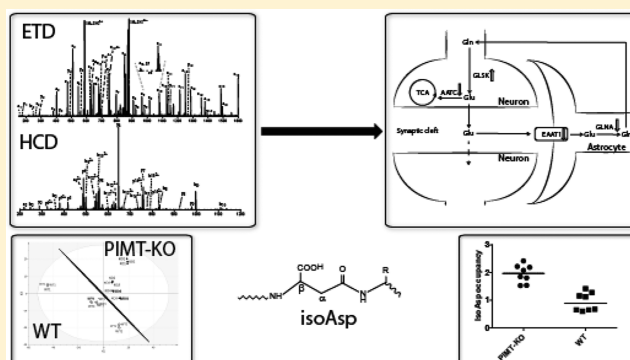
INTRODUCTION

Protein damage is believed to be one of the major processes in aging.[1] Natural proteins are subject to various types of damage, such as oxidation, deamidation and racemization of amino acid residues, and misfolding of the polypeptide chain. Although cells containing damaged proteins can be removed by the immune system, the level of damaged proteins within cells can also be reduced via lysosomal or proteasomal degradation or by molecular repair pathways. Protein L-isoaspartyl methyltransferase (PIMT) is a repair enzyme that initiates the conversion of the isoaspartyl residue (isoAsp), which is a major product of protein damage via asparagine (Asn) deamidation and aspartate (Asp) isomerization, to normal Asp residues.[2] The conversion occurs via isoAsp methylation using S-adenosyl-L-methionine (AdoMet) as the methyl donor, followed by cyclization and hydrolysis.[3] PIMT is a well-conserved enzyme in nature; it is expressed in almost all cells and tissues and is particularly highly expressed in brain.[4] PIMT-knockout (PIMT-KO) mice show growth retardation and perturbed glutamate metabolism and

usually die at less than 2 months of age from fatal seizures.[5] As expected, the level of isoAsp-containing proteins increases with time compared to that of wild-type (WT) controls: the abundance of brain isoAsp in 30- to 40-day-old PIMT-KO mice reaches around 1200 pmol/mg protein compared to 200 pmol/mg in WT mice.[5] Abnormalities of microtubule organization in the dendrites of pyramidal neurons have also been reported in PIMT-KO mice.[6] As the expression of PIMT is essential for survival, the substrates of PIMT under physiological conditions have been under intense investigation.[7−11] Because of the strong physiological response, there are reasons to suspect that the PIMT knockout affects important brain pathways.[5,6] Thus far, it has been reported that PIMT regulates p53 activity,[12] and the absence of methyltransferase results in activation of the insulin pathway[13,14] and MEK-ERK[15] pathway. To provide a deeper understanding of the molecular changes induced by the

PIMT deficiency, we performed here proteomics analysis of the whole PIMT-KO mouse brain. The goal of the analysis was twofold: (1) to examine the effect of PIMT on isoAsp content in previously reported and newly identified PIMT substrates and (2) to identify proteins with significantly altered abundances and to map them on metabolic pathways.

In previous studies, we have quantified isoAsp content with label-free shotgun proteomics in clinical samples (blood plasma of Alzheimer's disease [AD] patients)[16] and studied brains in an AD mouse model.[17] Here, as in previous work, we applied a filter-aided in-solution sample preparation (FASP) protocol that successfully deals with the problem of the large lipid content of the brain.[18] Proteomics findings are typically validated by an orthogonal approach (e.g., Western blot or ELISA). However, immunological validation works best when the changes in protein abundance reach a level of 50% or more, whereas here we aimed to detect smaller abundance variations in an unbiased manner. Therefore, to corroborate the findings provided by FASP proteomics, we performed, as in the previous work, an additional proteomics analysis using a different sample preparation method: protein in gel digestion. Such a validation approach, although not fully orthogonal to the discovery method (mass spectrometry was used in both analyses for protein identification and quantification), is still satisfactory because of the complementary nature of FASP sample preparation compared to that of gel-based methods. Indeed, the peptides detected with these two approaches are often different, although they originate from the same proteins.[19]

The detection of isoAsp residues has traditionally relied on the immunological assay or PIMT-based enzymatic assay.[20] The recent emergence of electron capture dissociation (ECD) and electron transfer dissociation (ETD) has led to the ability of tandem mass spectrometry (MS/MS) to differentiate isoAsp from Asp residues by a "signature" fragment of (z - 57 Da).[21] However, additional filtering based on the evaluation of the tandem mass spectra as well as the chromatography profiles of the eluting peptides is required to reach a high level of specificity in proteome-wide isoAsp analysis.[22,23] Another problem is in vitro isoAsp production. Proteomics sample preparation, especially protein digestion, often induces Asn deamidation and thus generates isoAsp residues (at moderate levels of 3−5%).[23] At the same time, Asp isomerization leading to isoAsp is a much slower process,[24] and thus it is mostly induced in vivo. To track the isoAsp contents introduced in vitro, 18O labeling sample preparation procedures have been developed.[25−27] In the previous study of blood plasma proteins, we investigated only isomerization-produced isoAsp because of the low level of isoAsp in human blood.[16] In the present study, higher levels of isoAsp are expected in the PIMT-KO mouse brain cells,[4,5] which reduces the concern over in vitro deamidation. Even if some deamidation occurs during sample preparation, a higher level of isoAsp residues at a particular site in a PIMT-KO protein relative to its WT counterpart will indicate that this isoAsp is a physiological substrate of PIMT. Therefore, we investigated here isoAsp residues originating from both deamidation and isomerization processes. Using shotgun proteomics, we have presented the brain isoaspartome for the first time.

■ EXPERIMENTAL SECTION

PIMT-Knockout Mice

As described previously, PIMT knockout mice ($Pcmt1^{-/-}$) with a background of 50% C57BL/6 and 50% 129/Sv were generated by breeding heterozygous $Pcmt1^{\pm}$ mice that had been inbred for over 15 years.[5] These mice were treated in accordance with animal use protocols approved by the UCLA Animal Research Committee (protocol 1993-109). Eight young female mice (four $Pcmt1^{-/-}$ and four $Pcmt1^{+/+}$, 51 to 53 days old) were decapitated. The brain was removed as quickly as possible, cut in half with a razor blade, and dropped into liquid nitrogen. The frozen brains were then stored at −80 °C until further analysis. Genotyping by PCR was performed both prior to weaning and after dissection to confirm each animal's identification.[5] The sample name, gender, type, and age of the mice used are listed in Table S1.

Brain Proteome Extraction

Protein extraction buffer containing 62.5 mM Tris-HCl (pH 6.8), 2% sodium dodecyl sulfate (SDS), 10 mM dithiothreitol (DTT), and 10% glycerol was added to the tissue corresponding to 10 times the wet weight (e.g., 10 μL buffer for a 1 mg sample). The tissue samples were vortex mixed and incubated on ice for 5 min. Then the tissues were homogenized on ice by TissueRuptor (QIAGEN) and sonicated on ice for 2 s with a 1 s pause, with a total sonication time of 100 s. The samples were then incubated for 10 min at 70 °C with a shaking frequency of 1400 Hz. Tissue debris was removed by centrifugation at 16 000g for 15 min. The protein concentration for each supernatant was determined by the BCA protein assay (Thermo Scientific Pierce) according to the protocol provided by the producer.

Filter-Aided Sample Preparation (FASP)

Protein extracts were digested with trypsin as described previously.[18] Briefly, 10 μg of tissue sample was reduced for 10 min with 5 mM DTT in 50 mM ammonium bicarbonate (AmBic) solution at 90 °C. Then the entire solution was transferred onto a 30 kDa Nanosep Ultrafiltration device (PALL), and the samples were washed twice with 8 M urea in 50 mM AmBic (UA solution) with centrifugation. Incubation at room temperature in the dark with 50 mM iodoacetamide (IAA) in UA solution was used for protein alkylation. Sequencing Grade Modified Trypsin (Promega) was used for protein digestion with an enzyme/substrate ratio of 1:50. The samples were incubated overnight at 40 °C, and the final digests were obtained in a solution of 0.5 M NaCl in 5% formic acid (FA). These solutions were desalted by ZipTip (Millipore), dried by SpeedVac, and stored at −20 °C until further analysis.

SDS-Polyacrylamide Gel Electrophoresis (SDS-PAGE) Separation

To eliminate the large lipid content of the brain that otherwise risked contaminating the chromatographic equipment, protein extracts (30 μg of protein per lane) were separated by NuPAGE Novex Bis-Tris Mini Gels (Invitrogen). After protein separation, the gel was stained with 0.1% Coomassie Brilliant Blue R-250 solution.

Protein-in-Gel Digestion

Each gel lane was cut into 15 pieces of approximately equal size. The gel pieces were incubated in destaining solution (50% acetonitrile (ACN) in 50 mM AmBic solution) at 40 °C for 10 min. After the destaining procedure was applied twice, the gel

pieces were soaked in 100% ACN and incubated at 40 °C until totally dehydrated. Incubation with 10 mM DTT at 40 °C for 30 min followed by 55 mM IAA at 40 °C for 20 min was used for protein reduction and alkylation. Sequencing Grade Modified Trypsin (Promega) was used for protein digestion with an enzyme/substrate ratio of 1:10. The samples were incubated overnight at 40 °C. The digestion was stopped with 1% FA, and the digested peptides were extracted with 1% FA in 50% ACN. The samples were then cleaned with ZipTip (Millipore). Samples from the same lane were pooled together, dried by SpeedVac, and treated afterward as one sample. Dried samples were stored at −20 °C until further analysis.

Mass Spectrometry (MS) Analysis

Protein digests (0.5 μg, resuspended in 0.1% FA) were loaded into a 25-cm-long column (New Objective) home-packed with 3 μm C_{18} beads. Peptides were separated with a 120 min gradient (buffer A, 0.1% FA; buffer B, 0.1% FA in ACN) on an Easy-nLC system (ThermoFischer Scientific). The LC gradient started eluting from 5% buffer B to 40% buffer B in 90 min, increased to 95% buffer B in 5 min, and then continued to elute at 95% buffer B for 10 min. A Velos Orbitrap mass spectrometer (ThermoFisher Scientific) was used with a MS survey scan at a resolution of $R = 60\,000$, and the five most abundant peaks were selected with a mass window of 3 m/z units for MS/MS fragmentation in the Velos LTQ ion trap by collision induced dissociation (CID) and electron transfer dissociation (ETD). Three technical replicate analyses of each FASP digested sample were performed, two of them with both CID and ETD MS/MS and one analysis with only CID MS/ MS. Therefore, only two of these technical replicates provided information about the presence of isoAsp. Finally, each in-gel digestion was analyzed by LC-MS once with both CID and ETD MS/MS.

Data Processing

Peak List Generation and Database Searches. MS/MS spectra were extracted, charge state deconvoluted, and deisotoped using home-written program RAW_to_MGF version 2.0.5, which also limited each MS/MS spectrum to its 200 most intense peaks. Then, MS/MS spectra from different runs were merged using home-written program Cluster_MGF to make one .MGF file for FASP-digested samples and one .MGF file for in-gel-digested samples. Cluster_MGF gathers groups of MS/MS spectra that share N of the 20 most-intense fragment peaks (N is usually 10). These groups are presumed to originate from MS/MS of the same peptide. The spectrum in each group that has the maximum aggregate intensity is taken as a representative of this group for storage in the .MGF file, whereas other MS/MS spectra are discarded.[28] This procedure greatly reduces the size of the resultant .MGF file and the time required for its subsequent matching to a MS/MS database performed by the Mascot search engine (Matrix Science, London, U.K., version 2.3.02). The search was performed separately for CID and ETD MS/MS data, with a precursor mass window of 10 ppm, an MS/MS window of 0.6 Da, a maximum of two missed tryptic cleavages, and carbamidome-thylation of cysteine as a fixed modification. Asparagine and glutamine deamidation and methionine oxidation were allowed as variable modifications. (The inclusion of these variable modifications made sequence assignment more reliable.) The database search was performed against the UniProt_Comple-te_Proteomes_Mus_V_06−03−2013 database concatenated with the decoy reverse-sequence compilation of this database

for false discovery rate (FDR) determination (containing 42 793 sequences plus an equal number of the reversed sequences).

Criteria for Protein Identification. Scaffold (version Scaffold_4.0.3, Proteome Software Inc., Portland, OR) was used to improve the accuracy of MS/MS-based peptide and protein identification. Peptide identification was accepted if it was deemed by the Scaffold Local FDR algorithm to have greater than 95% reliability. Protein identification containing at least two identified peptides was accepted with a greater than 99% probability. Protein probabilities were assigned by the Protein Prophet algorithm.[29] Proteins that contained similar peptides and could not be differentiated on the basis of MS/MS analysis alone were grouped to satisfy the principles of parsimony. Proteins sharing significant peptide evidence were pooled into clusters.

Protein Quantification. Label-free quantification of the proteins was performed by home-written program Quanti, version 2.5.3.1.[28] This program integrates extracted ion chromatograms (XICs) of peptides identified by Mascot and considers all charge states and available isotopic peaks of the molecular ions. Quanti uses for quantification only reliably identified (FDR < 0.01), first-choice, unmodified, unique-sequence peptides. No fewer than two such peptides have to be present for a protein to be quantified. If two protein entries have partial sequence overlap, then all of the peptides belonging to this overlap are excluded from quantification.

Statistical Analysis. The quantified proteome results were analyzed by SIMCA software (version 13.0.0.0, Umetrics AB, Sweden) via principal component analysis (PCA).

Bioinformatic Functional Analysis. Functional analysis was performed using the DAVID (Database for Annotation, Visualization and Integrated Discovery, version 6.7) Bio-informatics Resource. Proteins identified as differentially expressed between control and PIMT-KO mice were assessed by Gene Ontology (GO) for significant enrichment of biological processes.

Isoaspartate Identification and Quantification. IsoAsp content was analyzed by home-written software Isoaspartatics, version 1.1.6, which looked for Asn deamidation and Asp isomerization by the presence of $(z - 57\ \mathrm{Da})$ ions in the ETD MS/MS spectra. Identification of an isoAsp site required that the $(z - 57\ \mathrm{Da})$ ion did not overlap with any theoretical m/z for c or z ions and matched the expected mass with a tolerance of 0.1 Da. IsoAsp-containing peptides were quantified on the basis of their extracted ion chromatograms, which required baseline chromatographic separation between the native and modified peptides. Additional criteria, such as MS/MS identification of the native Asp form of the isoAsp-containing peptide and observation of the isotopic peak of the $(z - 57\ \mathrm{Da})$ ions, were applied to substantiate further the presence of an isoAsp residue.

■ RESULTS

IsoAsp Identification and Quantification

Our first goal was to use mass spectrometry to identify proteins that contain isoAsp residues in WT mouse brains and in brain proteins from mice lacking isoAsp-repair methyltransferase, PIMT. The presence of the signature $(z - 57\ \mathrm{Da})$ ions appears to be specific for the identification of the subtle posttransla-tional modification (CH_2 group rearrangement from the side chain to the backbone) accompanying isoaspartyl forma-
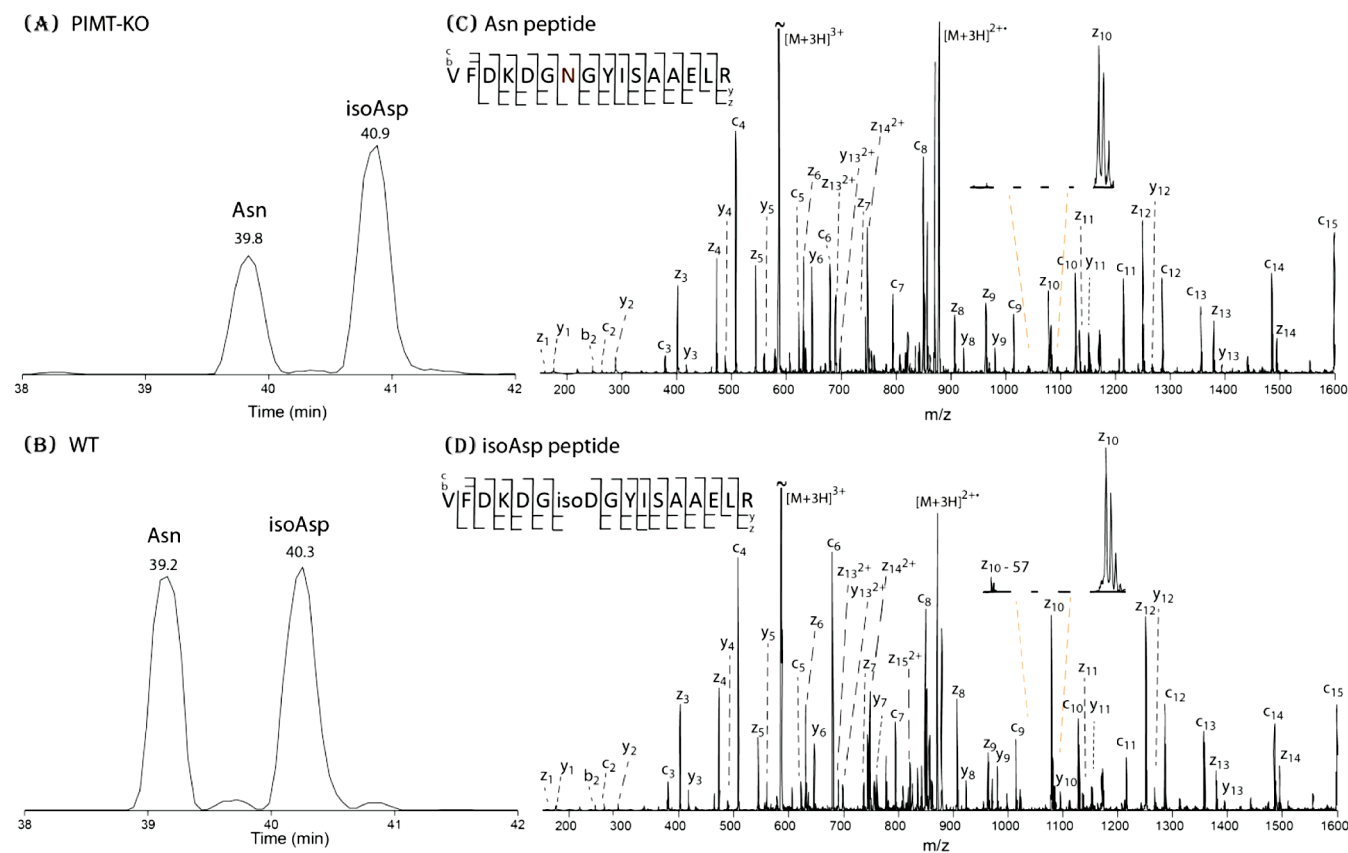
Figure 1. (Left) Extracted ion chromatographic profiles of 3+ ions of peptide [92]VFDKDG**N**GYISAAEL[107]R (Asn) from calmodulin and its deamidated form [92]VFDKDG**isoD**GYISAAEL[107]R (isoAsp). (A) PIMT KO mice. (B) WT mice. (Right) ETD MS/MS spectrum of 3+ ions. (C) [92]VFDKDG**N**GYISAAEL[107]R (Asn) native peptide. (D) [92]VFDKDG**isoD**GYISAAEL[107]R (isoAsp) peptide. The inset shows the absence or presence of $(z - 57 \text{ Da})$ ions.

tion.[16,22] In the present study, we selected isoAsp-containing peptide candidates only if the peptides were successfully identified and quantified in all FASP digested samples and the signature ion was present in both FASP digestion technical replicates. Using these stringent criteria, we detected 67 unique isoAsp-containing peptides. In peptides from PIMT-KO mouse brain proteins, 12 isoAsps originated at sites of asparagine deamidation and 36 arose from the isomerization of aspartyl residues. In peptides from WT control brain proteins, 11 isoAsps originated at sites of asparagine deamidation and 33 arose from the isomerization of aspartyl residues. Nine of the 14 isoAsp sites resulting from deamidation were common to proteins from both WT and PIMT-KO animals, and 16 of the 53 isoAsp sites generated by aspartyl residue isomerization were found in both WT and KO brains (Tables S2−S5). The absence of the repair methyltransferase in PIMT-KO mouse brain has previously been shown to result in an accumulation of isoAsp residues, and 23 sites of isoAsp formation were found here solely in the PIMT-KO mouse brain proteins. Surprisingly, however, an additional 19 unique isoAsp sites were found in WT but not in KO brain proteins. The appearance of isoAsp sites in WT but not in KO mice could be a spurious result of insufficient statistics in isoAsp detection by MS/MS. The difference between the isoAsp spectral counts in PIMT-KO and WT mice, although in favor of PIMT-KO, was too small to be statistically significant. Thus, an alternative to the MS/MS spectral counting method was needed to assess the relative isoAsp levels in these groups.

In principle, the Quanti program is capable of quantifying all of the variants of each peptide in the data set. However, this required reliable chromatographic separation between the native and isoAsp peptides, which was not always the case. Because the main goal was to assess the general isoAsp level in PIMT-KO and WT brains, whereas individual peptide data were less important, we selected as representative two peptides with well-separated chromatograms and reliable MS/MS identification of both native and isoAsp-containing peptides and the presence of the isotopic distribution of the $(z - 57 \text{ Da})$ ion. The relative abundances of the variants were quantified by their XICs.

After quantification, the difference between the PIMT KO and WT mice became more apparent. Among the 19 isoAsp sites uniquely identified by MS/MS in WT mice, none of the 17 peptides with isomerization-induced isoAsps (which to a higher degree than deamidation-generated isoAsps are due to in vivo accumulation) showed significantly different levels in WT versus KO. At the same time, among the 23 sites unique to the KO mouse, 2 out of 20 isomerization-induced isoAsp sites (Table S6) showed high significance $(p < 0.001)$: LDLIAQQMMPEVR from V-type proton ATPase subunit E1 (the KO/WT abundance ratio = 1.29) and VDNDE-NEHQLSLR from nucleophosmin (the KO/WT abundance ratio = 1.32).

Even more apparent was the difference among the levels of peptides with isoAsp detected by MS/MS in both types of mice or only in KO mice. To demonstrate this difference, we chose two peptides with chromatographically well-separated isoAsp
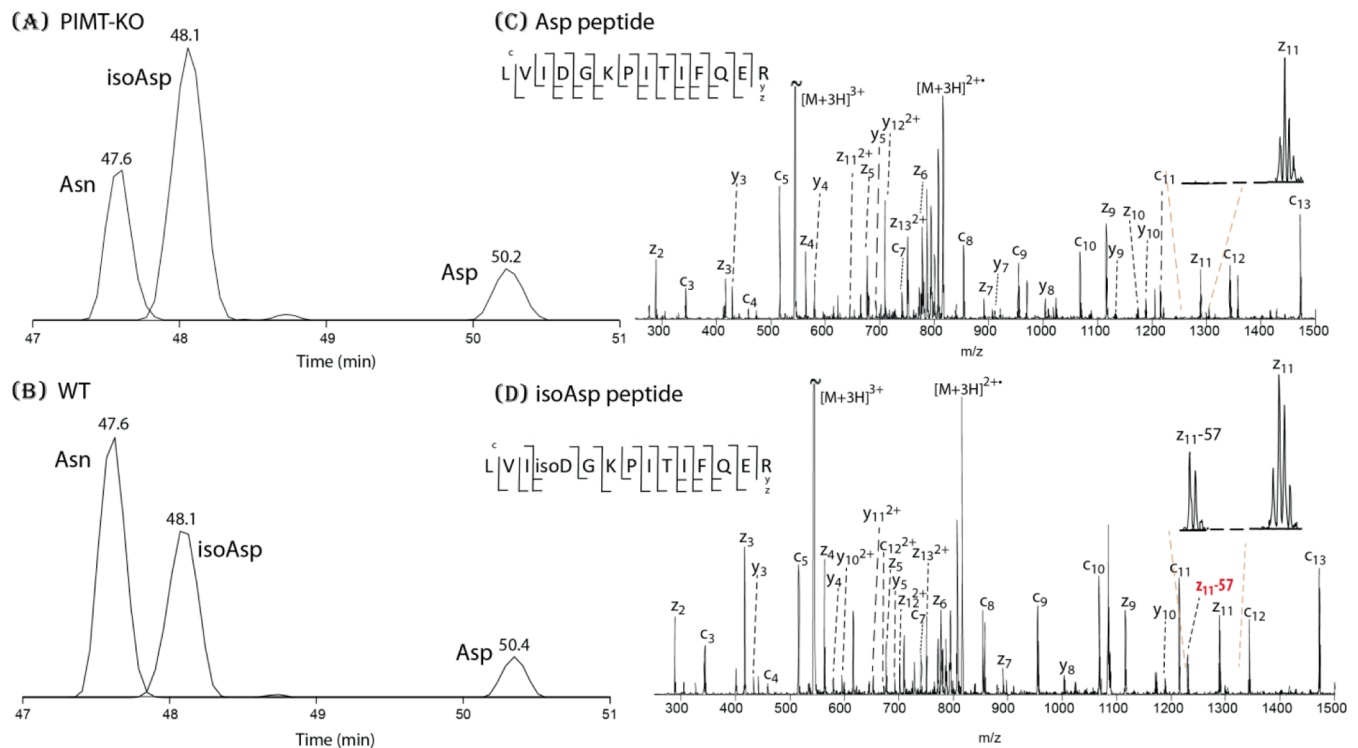
Figure 2. (Left) Extracted ion chromatographic profiles of 3+ ions of peptide [65]LVI**N**GKPITIFQE[78]R (Asn) from glyceraldehyde-3-phosphate dehydrogenase and its deamidated forms [65]LVI**D**GKPITIFQE[78]R (isoAsp) and [65]LVI**D**GKPITIFQE[78]R (Asp) in samples of (A) PIMT KO mice and (B) WT mice. (Right) ETD MS/MS spectrum of 3+ ions of (C) the [65]LVI**D**GKPITIFQE[78]R (Asp) peptide and (D) [65]LVI**isoD**GKPITIFQE[78]R (isoAsp) peptide. The inset shows the absence or presence of $(z - 57$ Da$)$ ions.

and native variants; the ratio of abundances of these variants provided the estimate for the isoAsp occupancy. The measurements of occupancies (stoichiometries) made with two replicate proteomic analyses of each of the eight mice (four mice of each type) allowed for a reliable statistical evaluation of the results.

The two investigated peptides were [92]VFDKDG**N**GYI-SAAEL[107]R from calmodulin (Figure 1) and [65]LVI**N**GKPI-TIFQE[78]R from glyceraldehyde-3-phosphate dehydrogenase (Figure 2). The relatively large amount of isoAsp observed in the peptides generated from the WT mouse proteins suggests that these Asn residues are particularly labile and may have deamidated during the proteolytic digestion and processing. The larger relative abundance of isoAsp residues in the comparable peptides from PIMT-KO proteins, however, indicates how many of these sites might be repaired by PIMT in vivo. The isoAsp occupancy of [92]VFDKDG**N**GYI-SAAEL[107]R in PIMT-KO mice was almost 2 times the quantity in WT controls ($p < 0.01$ in the two-tailed Student's t test) Figure 3(A). Zero counts in Figure 3 correspond to the cases in which the quantification program could not reliably attribute any XIC in the LC/MS data set to the corresponding peptide. The isoAsp occupancy of [65]LVI**N**GKPITIFQE[78]R in PIMT-KO mice was somewhat more than 2 times that in WT controls ($p < 0.001$ in the two-tailed Student's t test, Figure 3B). Here, the average abundance ratio of isoAsp and Asp variants is 4.6 for PIMT KO and 3.6 for WT mice, which is consistent with isoAsp repair by PIMT and its conversion to Asp. The quantification data for these two modified peptides are given in Table S7.
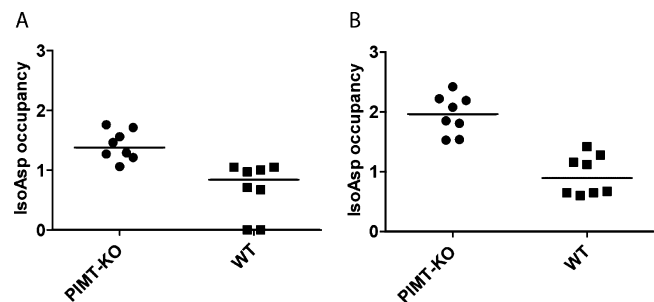

Figure 3. IsoAsp occupancy (ratio of the isoAsp/native peptide abundances) in (A) calmodulin peptide VFDKDG**N**GYISAAELR and (B) glyceraldehyde-3-phosphate dehydrogenase peptide LVI**N**GKPI-TIFQER in four PIMT-KO mice and four WT controls measured in two replicate FASP-based proteomic analyses. Lines indicate the median value in each data set.

Protein Identification and Quantification by FASP

Although it is likely that the increase in isoAsp levels in PIMT-KO mice contributes to the observed phenotype, it remains unclear what other cellular changes might be contributing to this phenotype. To determine whether expression levels of critical proteins were altered by the absence of PIMT, we identified by the FASP method 5768 peptides belonging to 832 proteins with FDR < 1% (Tables S8 and S9) and were able to quantify 811 of these proteins (Table S10). Two-dimensional PCA analysis (SIMCA, $R^2X[\text{cum}] = 0.912$; $Q^2[\text{cum}] = 0.785$) successfully separates this data set into two groups: WT controls and PIMT-KO mice (Figure 4). Then the two-tailed Student's t test was applied to select the proteins that were significantly altered in PIMT-KO compared to the WT controls. The threshold p value was chosen to be <0.001;
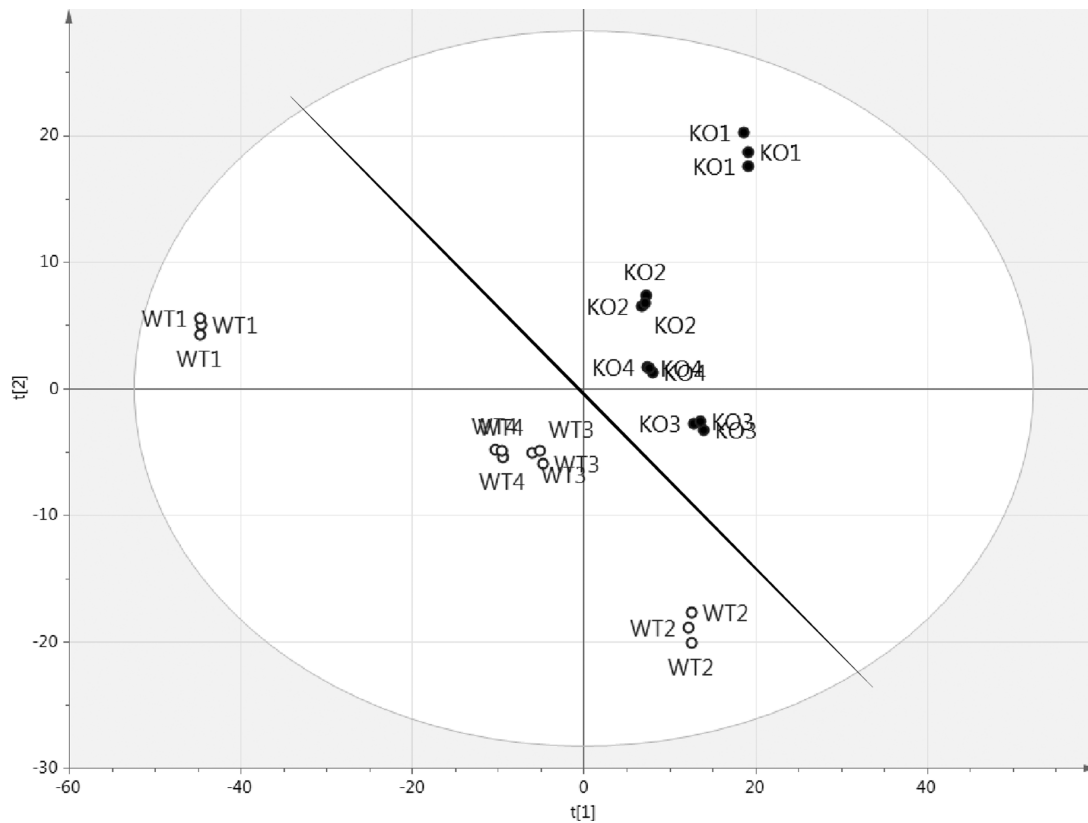
Figure 4. Principal component analysis (PCA) of protein abundances from the whole-brain proteome analysis performed by FASP digestion (SIMCA, $R^2X[cum] = 0.912$; $Q^2[cum] = 0.785$): black circles (KO), PIMT-KO mice; white circles (WT), wild-type controls. The line separates the data set into two groups, PIMT-KO and WT.

Table 1. Proteins Whose Expression Levels Are Significantly Altered by the Absence of the Isoaspartyl Methyltransferase in PIMT-KO Mice Compared to WT Controls as Found by Both FASP ($p < 0.001$) and in-Gel ($p < 0.005$) Methods of Proteomic Analysis

protein id	description	FASP		in-gel	
		p value	fold KO/WT	p value	fold KO/WT
CAMKV_MOUSE	CaM kinase-like vesicle-associated protein	4.01×10^{-04}	1.8	3.37×10^{-04}	2.7
GLSK_MOUSE	glutaminase, kidney isoform l	7.13×10^{-09}	1.4	1.29×10^{-03}	1.9
PCBP2_MOUSE	poly(rC)-binding protein 2	9.15×10^{-05}	0.8	3.01×10^{-03}	0.7
DX39B_MOUSE	spliceosome RNA helicase	4.01×10^{-04}	0.8	4.75×10^{-03}	0.8

thus, less than 1 false significant protein was expected in the whole data set containing 811 proteins. The analysis resulted in 182 significantly altered proteins (Table S11), including PIMT that was found as the 725th most abundant protein in WT samples and absent in PIMT KO mice (Figure S1).

Protein Identification and Quantification by in-Gel Digestion

To validate the results found with the FASP method described above, we next used a different protein preparation technique, gel-based separation and in-gel digestion, to generate peptides for MS analysis. In total, 4628 unique peptides belonging to 796 proteins were identified with an FDR of <1% (Tables S12 and S13). With a minimum of 2 unique peptides, 790 of these proteins were quantified (Table S14). Although in-gel digestion provides less-accurate data than FASP in label-free quantification because of multiple steps involving protein or peptide losses, PCA analysis was still able to separate the two groups of mice (Figure S2A). Most of the significantly regulated proteins found in FASP (90%) were also quantified using the in-gel

digested sample. Among the 163 significantly regulated proteins quantified by both methods, 151 proteins (93%) had the same regulation direction in both analyses (Table S15, Figure S2B,C). Using $p < 0.005$ as a significance cutoff threshold for the in-gel method (for 151 proteins, $p < 0.005$ guarantees on average less than 1 false significant protein), we determined the most reliably identified significantly regulated proteins (Table 1).

Bioinformatic Functional Analysis

Our final goal here was to determine what specific changes in protein levels observed in the PIMT-KO mouse brain could contribute to the phenotype observed in these mice. Among the most reliable 151 significant proteins (Table S15), 83 are up-regulated in PIMT-KO mice and 68 are down-regulated. Using all identified proteins as a background data set (Table S16) and $p < 0.001$ as a significance threshold, gene ontology (GO) analysis was performed. The analysis of proteins down-regulated in PIMT-KO mice yielded cellular amino acid biosynthesis as the only significantly enriched process ($p =$

0.0008). Thus, this process is likely to be suppressed in PIMT-KO brains compared to WT. Up-regulated in PIMT-KO mice proteins did not yield any process with statistical significance.

■ DISCUSSION

Isoaspartome Regulated by PIMT

Protein deamidation and isomerization are spontaneous reactions both in vitro and in vivo. The reaction rates for these modifications are influenced by the primary sequence and 3D structure as well as by the temperature, pH, and ionic strength of the solution. Therefore, the in vitro deamidation rate can be approximately predicted in silico using a computational model built with the help of extensive experimental data.[30] In the pharmaceutical industry, minimizing deamidation and isomerization during drug production, formulation, and storage is of great importance.[31] Under physiological conditions, isoAsp residues arising at specific sites by deamidation and isomerization can have regulatory functions, such as in the response to DNA damage[32] and in p53 stability.[12] High isoAsp levels have a negative impact on mammalian tissues (e.g., they can affect the crystal structure of the human lens[33] and induce an autoimmune response[34]). Therefore, isoAsp formation and the PIMT repair capability play essential roles in both cellular regulation and protein aging processes.

Until recently, isoAsp identification and quantitation have mostly been carried out with the ISOQUANT isoaspartate detection kit, which uses recombinant PIMT to radiolabel isoAsp residues with *S*-adenosyl-[3*H*-methyl]-methionine.[35] Two recent reports use this assay, combined with 2D electrophoresis and blotting on membranes, to isolate isoAsp-containing proteins from PIMT-KO mouse brains.[7,11] When methylation was performed first, followed by electrophoresis, blotting, and MS, 12 isoAsp-containing proteins were identified,[7] though this technique might have lost the most labile methyl esters during the purification procedure.[36] When the enzymatic methylation was instead performed after the proteins had been separated and blotted onto a membrane, 19 isoAsp-containing proteins were identified,[11] though some of these isoAsps may be new nonphysiological sites that were generated during the procedure. The difference between these procedures is illustrated by the fact that only α- and β-tubulin were identified in both reports as containing isoAsp residues. In contrast to these previous reports, we have used the recent discovery of a specific ($z - 57$ Da) fragment ion of isoAsp in ECD/ETD MS/MS spectra[21] and the procedures described in this current study to detect a total of 67 isoAsp-containing proteins. Four of the 12 isoAsp-containing proteins found by Vigneswara et al.,[7] including clathrin light chain A and calmodulin, and 9 of the 19 isoAsp-containing proteins found by Zhu et al.,[11] including synapsins I and II, are confirmed here, and now we have identified a specific site of damage in each of these proteins.

The fact that we observed 3 times more isoAsp residues in WT and PIMT-KO proteins arising from aspartyl isomerization than from asparaginyl deamidation is quite surprising. In one previous report, the rates of isoAsp formation measured in vitro in small synthetic peptides were found to be 6.5 to 21 times faster at Asn sites than from the corresponding Asp sites at 37 °C, pH 7.4.[37] Our results here support the idea that isoAsp formation from Asn deamidation is limited by native protein structure in the mouse brain whereas isoAsp formation from Asp isomerization is perhaps promoted by the structure of these proteins.

In addition to identifying labile asparaginyl and aspartyl residues in mouse brain proteins, we also wanted to know which sites are repaired by PIMT within brain cells. When repair is occurring, the isoAsp occupancy at a particular site will be lower in the WT brain than in the PIMT-KO brain. This will be observed even if deamidation during the experimental procedure generates new isoAsp residues because in vitro deamidation will occur equally in the PIMT-KO and WT proteins. Rather than using the enzymatic assay, the amount of isoAsp can now be quantified by specific fragment abundance,[38] counts of MS/MS spectra containing the signature fragment,[18] the targeted multiple reaction monitoring (MRM) assay,[23] or label-free quantification based on XIC.[22] In the present study, we used XIC to quantify two isoAsp-containing peptides that have clear baseline chromatographic separation between the native and isoAsp variants and excellent MS/MS data.

Peptide [92]VFDKDG**N**GYISAAEL[107]R containing isoAsp-98 originates from calmodulin, located in the calcium binding loop of the EF hand (domain III). Calmodulin contains four EF hand domains, and each of the domains can bind calcium. Interestingly, the domain with Asn-98 has the highest calcium binding affinity among all domains.[39] The transformation of Asn-98 to Asp-98 or isoAsp-98 in calmodulin results in losses of 60 and 90% protein activity, respectively.[2] The detection of isoAsp-98 is not surprising: Asn-98 was found to be the most susceptible site for isoAsp formation during in vitro protein aging.[39] Previously, only low levels of isoAsp had been identified in calmodulin from PIMT-KO mouse brains.[10] Although much of the isoAsp that we observe at this labile site may have arisen during in vitro processing, the differences in PIMT-KO versus WT isoAsp levels between these studies may reflect the different efficiencies of the two techniques of isoAsp quantification for this specific deamidation site of calmodulin. Almost twice as much isoAsp was found in this calcium-binding domain in PIMT-KO compared to that for WT mice. Lower calcium-binding activity of isoAsp-containing calmodulin molecules may disturb the downstream calmodulin-dependent pathways.

Another peptide with a higher isoAsp level in PIMT-KO mice, [65]LVI**N**GKPITIFQE[78]R containing isoAsp-68, belongs to glyceraldehyde-3-phosphate dehydrogenase (GAPDH). To our knowledge, this is the first time that GAPDH has been identified as an in vivo substrate for PIMT. GAPDH is an important housekeeping enzyme, and its involvement in glycolysis has been well studied. Other biological functions, such as membrane fusion, have also been associated with GAPDH.[40] In in vitro experiments, the main deamidation site of GAPDH has been localized in the N-terminal peptide ([2]VKVGVNGFG[11]R), where the structure is quite constrained.[41] Asn-68 has not been reported previously as a major deamidation site. The domain that contains peptide [65]LVI**N**GKPITIFQE[78]R has no known catalytic activity, but it can bind tryptophanyl-tRNA synthetase.[42] This domain can also contribute to the membrane fusion function.[40] The biological effects of the deamidation of Asn-68 in GAPDH are unclear but may result in the reduction of the above functions.

As described above for calmodulin, the true isoAsp levels in both proteins are likely to be somewhat lower than measured as a result of the almost inevitable in vitro deamidation occurring during sample preparation. This artifact is relatively more

important for WT mice, where isoAsp levels are lower. Therefore, the true isoAsp occupancy change due to the absence of repair in PIMT-KO cells is likely to be much higher than the factor of 2 obtained here and thus closer to the factor of 6 measured in crude mouse brain preparations in the previous study by enzymatic methylation.[5]

Altered Proteome and Pathways

Although all of the new isoAsp sites discovered here will need to be quantitated and their effects on protein function will need to be assayed to determine their specific roles in mouse brain cell function, we can also examine their cumulative effect on cellular metabolism by examining how protein expression levels are altered in PIMT-KO cells. The four proteins with the most significantly altered expression levels (two up-regulated and two down-regulated) are given in Table 1.

Protein CAMKV (CaM kinase-like vesicle-associated protein) that is up-regulated 1.8- to 2.7-fold in PIMT-KO mice is considered to be catalytically inactive, but it may, according to UniProt, play a role in vesicle function and nervous system development. One proteomic study on the Ercc1 mouse model, which has a DNA repair deficiency and thus exhibits accelerated aging, has reported significant up-regulation of this protein.[43] Because CAMKV shares sequence similarities with Ca^{2+}/ calmodulin-dependent protein kinase, it could also be important for Ca^{2+} homeostasis.

Protein GLSK (glutaminase, kidney isoform) is up-regulated in PIMT-KO mice as well (1.4- to 1.9-fold). Both the kidney isoform (GLSK or GLS1) and liver isoform (GLS2) of glutaminase are expressed in the brain.[44] Glutaminase catalyzes the conversion of glutamine to glutamate. Glutamate is one of the main neurotransmitters, and 70% of the glutamate used in neurotransmission is generated through the glutamine–glutamate pathway with the help of GLSK.[45] Although GLSK knockout is fatal for mice, glutamatergic synaptic transmission in cultured GLSK-KO cortical neurons is normal. Therefore, compensation for minor glutamate-generating pathways seems to be present in neurons, such as the transamination of α-ketoglutarate with alanine, branched-chain amino acids, and lysine, that maintain glutamatergic synaptic transmission.[45]

PCBP2 (poly(rC)-binding protein 2), down-regulated 0.7- to 0.8-fold in PIMT-KO mice, is essential for mRNA stability and translational controls (silencing and enrichment).[46] PCBP2 is also involved in innate immunity acting as a negative regulator in MAVS-mediated antiviral signaling. The expression of PCBP2 is significantly altered upon viral infection.[47] Because the down-regulation of PCBP2 is also found in hepatitis C virus (HCV)-replicon-containing cells, it is thought to have an antiviral effect on HCV.[48] Moreover, PCBP2 plays an important role in the stress response by binding with MAPKAP1 (mitogen-activated protein kinase associated protein 1).[49] Cells with down-regulation of either MAPKAP1 or PCBP2 are more susceptible to environmental stress, such as viral infection, inflammation shock, or oxidative stress.[49] Therefore, such a down-regulation of PCBP2 protein expression could reflect a weakened stress-responding system in PIMT-KO mice.

Another protein that is down-regulated (0.8-fold) in PIMT-KO mice is DX39B (spliceosome RNA helicase Ddx39b). DX39B is important for pre-RNA splicing and mRNA exportation from the nucleus to the cytoplasm.[50] The suppression of DX39B expression by RNAi causes the accumulation of a majority of the mRNAs inside the nucleus.[51]

In cardiomyocytes, the presence of DX39B and ATPase is essential to protein synthesis.[52] The down-regulation of DX39B that perturbs the mRNA expression process may contribute to the smaller size of the PIMT-KO mice,[4] as suggested before.[53]

To investigate which biological networks are most affected by PIMT knockout, the DAVID bioinformatics tool was used in mapping the 151 significantly regulated proteins (Table S15) to the gene ontology categories. The cellular amino acid biosynthetic process (GO: 0008652) was enriched with proteins down-regulated in PIMT-KO mice (p = 0.0008). Among these proteins, glutamine synthetase (GLNA) is involved in glutamine generation, aspartate aminotransferase (AATC) is involved in glutamate oxidation, excitatory amino acid transporter 1 (EAAT1) is involved in glutamate transportation, and D-3-phosphoglycerate dehydrogenase (SERA) and phosphoserine aminotransferase (SERC) are involved in serine biosynthesis.

At this point, it becomes apparent that the glutamate–glutamine cycle in CNS is significantly disturbed in PIMT-KO mice, which agrees well with previous knowledge.[5] Glutamate is the major excitatory neurotransmitter. After presynaptic release, the majority of glutamate is transported via EAAT1 into astrocytes, where glutamate is converted into glutamine via GLNA (Figure 5).[54] Then glutamine is transported back into
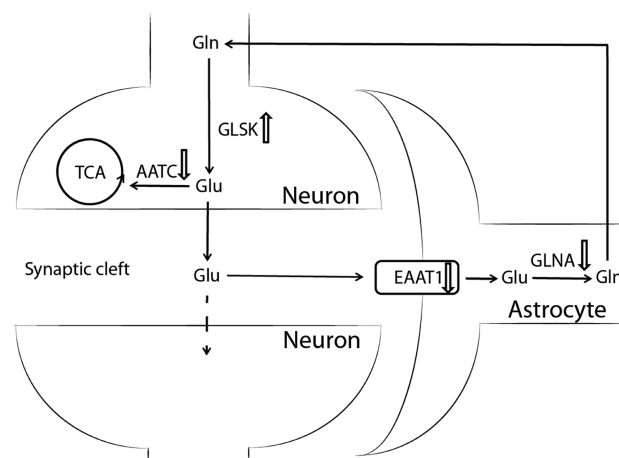

Figure 5. Glutamate–glutamine cycle in the central nervous system. Glutamate (Glu) is synthesized from glutamine (Gln) by glutaminase (GLSK) in the presynaptic neurons and released into the synaptic cleft. Besides being taken up by the postsynaptic neurons, the majority of Glu is transported by excitatory amino acid transporters (EAAT) into nearby astrocytes, where it is converted into Gln by glutamine synthetase (GLNA). Then Gln is released by astrocytes into the extracellular matrix and taken up by neurons, where it re-enters the cycle. At the same time, Glu can be oxidized into α-ketoglutarate and enter the tricarboxylic acid (TCA) cycle via aspartate aminotransferase (AATC). The arrows beside the protein names show their up- or down-regulation found in the current experiment. Figure adapted from Daikhin et al.[55]

the neurons and converted to glutamate via GLSK. At the same time, the brain oxidizes glutamate via AATC, continuously generating aspartate and 2-oxo-glutarate.[55] In PIMT-KO mice, we observed the down-regulation of EAAT1, GLNA, and AATC but the up-regulation of GLSK. The net effects should be an increase in the level of glutamate, which is consistent with the previous observations of 30% more glutamate in synaptosomes of PIMT-KO mice.[5] Excessive glutamate excitatory signals have been associated with epilepsy,[56] thus

the dysregulated glutamate–glutamine cycle may account for the epileptic seizures and subsequently the untimely death of PIMT-KO mice.

SERA and SERC are the first two enzymes involved in the serine synthesis pathway, which is the primary source of serine biosynthesis in the brain.[57] Serine is mainly produced in astrocytes and plays an essential role in CNS function and development.[57] Besides being consumed in protein synthesis, serine is used for the generation of glycine and neurotransmitter D-serine as well as several neuronal membrane lipids.[57] Serine deficiency causes intractable seizures in patients.[57] A high level of serine synthesis has been found in some cancer cell lines and is associated with breast cancer.[58] Serine is also the main carbon donor, via homocysteine to S-adenosylmethionine, in methylation reactions.[59] Therefore, the down-regulation of serine synthesis enzymes might significantly affect the one-carbon methylation metabolism in PIMT-KO mice. In fact, this down-regulation could possibly be compensating for the increased S-adenosylmethionine and decreased S-adenosylhomocysteine that is observed in PIMT-KO mouse brains. Further investigation of this hypothesis, however, is needed.

CONCLUSIONS

Here we confirmed the ability of modern proteomics to investigate simultaneously the isoaspartome and protein expression levels using a standard, high-throughput, untargeted, label-free proteomics experiment. Overall, 67 novel as well as previously known isoAsp-containing sites were identified, and two sites were thoroughly quantified, providing additional verification of significant isoAsp accumulation in the PIMT-deficient brain. The biological effects of isoAsp accumulation in each of the identified proteins remain to be investigated further. The expression levels of a large number of quantified proteins (ca. 15%) were found to be significantly altered when compared to WT levels, suggesting large changes in the global brain proteome. GO mapping of the proteins with altered levels verifies the earlier finding that glutamate metabolism is the main metabolic process perturbed with the PIMT deficiency, supporting possible regulatory roles of the enzyme. Additional findings that require further validation indicate that PIMT mice may suffer from a serine deficiency.

ASSOCIATED CONTENT

Ⓢ Supporting Information

Quantification profiles of protein L-isoaspartyl methyltransferase. Overall performance of the in-gel digestion method. Mouse information. IsoAsp-containing peptide candidates. Peptides and proteins identified from the FASP and in-gel methods. This material is available free of charge via the Internet at http://pubs.acs.org.

AUTHOR INFORMATION

Corresponding Author

*E-mail: Roman.Zubarev@ki.se. Telephone: +46 8524 87594.

Notes

The authors declare no competing financial interest.

ACKNOWLEDGMENTS

REFERENCES

(1) Clarke, S. Aging as war between chemical and biochemical processes: protein methylation and the recognition of age-damaged proteins for repair. *Ageing Res. Rev* **2003**, *2*, 263−285.

(2) Johnson, B. A.; Langmack, E. L.; Aswad, D. W. Partial repair of deamidation-damaged calmodulin by protein carboxyl methyltransferase. *J. Biol. Chem.* **1987**, *262*, 12283−12287.

(3) Johnson, B. A.; Murray, E. D., Jr.; Clarke, S.; Glass, D. B.; Aswad, D. W. Protein carboxyl methyltransferase facilitates conversion of atypical L-isoaspartyl peptides to normal L-aspartyl peptides. *J. Biol. Chem.* **1987**, *262*, 5622−5629.

(4) O'Connor, C. M. Protein L-Isoaspartyl, D-Aspartyl O-Methyltransferases: Catalysts for Protein Repair. In *The Enzymes*; Steven, G. C., Fuyuhiko, T., Eds.; Elsevier: Amsterdam, 2006; Vol. *24*, pp 385−433.

(5) Kim, E.; Lowenson, J. D.; MacLaren, D. C.; Clarke, S.; Young, S. G. Deficiency of a protein-repair enzyme results in the accumulation of altered proteins, retardation of growth, and fatal seizures in mice. *Proc. Natl. Acad. Sci. U.S.A.* **1997**, *94*, 6132−6137.

(6) Yamamoto, A.; Takagi, H.; Kitamura, D.; Tatsuoka, H.; Nakano, H.; Kawano, H.; Kuroyanagi, H.; Yahagi, Y.; Kobayashi, S.; Koizumi, K.; Sakai, T.; Saito, K.; Chiba, T.; Kawamura, K.; Suzuki, K.; Watanabe, T.; Mori, H.; Shirasawa, T. Deficiency in protein L-Isoaspartyl methyltransferase results in a fatal progressive epilepsy. *J. Neurosci.* **1998**, *18*, 2063−2074.

(7) Vigneswara, V.; Lowenson, J. D.; Powell, C. D.; Thakur, M.; Bailey, K.; Clarke, S.; Ray, D. E.; Carter, W. G. Proteomic identification of novel substrates of a protein isoaspartyl methyltransferase repair enzyme. *J. Biol. Chem.* **2006**, *281*, 32619−32629.

(8) Lanthier, J.; Bouthillier, A.; Lapointe, M.; Demeule, M.; Béliveau, R.; Desrosiers, R. R. Down-regulation of protein L-isoaspartyl methyltransferase in human epileptic hippocampus contributes to generation of damaged tubulin. *J. Neurochem.* **2002**, *83*, 581−591.

(9) Young, G. W.; Hoofring, S. A.; Mamula, M. J.; Doyle, H. A.; Bunick, G. J.; Hu, Y.; Aswad, D. W. Protein L-isoaspartyl methyltransferase catalyzes in vivo racemization of aspartate-25 in mammalian histone H2B. *J. Biol. Chem.* **2005**, *280*, 26094−26098.

(10) Reissner, K. J.; Paranandi, M. V.; Luc, T. M.; Doyle, H. A.; Mamula, M. J.; Lowenson, J. D.; Aswad, D. W. Synapsin I is a major endogenous substrate for protein L-isoaspartyl methyltransferase in mammalian brain. *J. Biol. Chem.* **2006**, *281*, 8389−8398.

(11) Zhu, J. X.; Doyle, H. A.; Mamula, M. J.; Aswad, D. W. Protein repair in the brain, proteomic analysis of endogenous substrates for protein L-isoaspartyl methyltransferase in mouse brain. *J. Biol. Chem.* **2006**, *281*, 33802−33813.

(12) Lee, J. C.; Kang, S. U.; Jeon, Y.; Park, J. W.; You, J. S.; Ha, S. W.; Bae, N.; Lubec, G.; Kwon, S. H.; Lee, J. S.; Cho, E. J.; Han, J. W. Protein L-isoaspartyl methyltransferase regulates p53 activity. *Nat. Commun.* **2012**, *3*, 927.

(13) Farrar, C.; Houser, C. R.; Clarke, S. Activation of the PI3K/Akt signal transduction pathway and increased levels of insulin receptor in protein repair-deficient mice. *Aging Cell* **2005**, *4*, 1−12.

(14) MacKay, K. B.; Lowenson, J. D.; Clarke, S. G. Wortmannin reduces insulin signaling and death in seizure-prone Pcmt$^{-/-}$ mice. *PLoS One* **2012**, *7*, e46719.

(15) Kosugi, S.; Furuchi, T.; Katane, M.; Sekine, M.; Shirasawa, T.; Homma, H. Suppression of protein L-isoaspartyl (D-aspartyl) methyltransferase results in hyperactivation of EGF-stimulated MEK-ERK signaling in cultured mammalian cells. *Biochem. Biophys. Res. Commun.* **2008**, *371*, 22−27.

(16) Yang, H.; Lyutvinskiy, Y.; Soininen, H.; Zubarev, R. A. Alzheimer's disease and mild cognitive impairment are associated with elevated levels of isoaspartyl residues in blood plasma proteins. *J. Alzheimer's Dis.* **2011**, *27*, 113−118.

(17) Yang, H.; Wittnam, J. L.; Zubarev, R. A.; Bayer, T. A. Shotgun brain proteomics reveals early molecular signature in presymptomatic

mouse model of Alzheimer's disease. *J. Alzheimer's Dis.* **2013**, *37*, in press.

(18) Wiśniewski, J. R.; Ostasiewicz, P.; Mann, M. High recovery FASP applied to the proteomic analysis of microdissected formalin fixed paraffin embedded cancer tissues retrieves known colon cancer markers. *J. Proteome Res* **2011**, *10*, 3040−3049.

(19) Fischer, F.; Wolters, D.; Rogner, M.; Poetsch, A. Toward the complete membrane proteome - High coverage of integral membrane proteins through transmembrane peptide detection. *Mol. Cell. Proteomics* **2006**, *5*, 444−453.

(20) Yang, H.; Zubarev, R. A. Mass spectrometric analysis of asparagine deamidation and aspartate isomerization in polypeptides. *Electrophoresis* **2010**, *31*, 1764−1772.

(21) Cournoyer, J. J.; Pittman, J. L.; Ivleva, V. B.; Fallows, E.; Waskell, L.; Costello, C. E.; O'Connor, P. B. Deamidation: differentiation of aspartyl from isoaspartyl products in peptides by electron capture dissociation. *Protein Sci.* **2005**, *14*, 452−463.

(22) Yang, H.; Fung, E. Y. M.; Zubarev, A. R.; Zubarev, R. A. Toward proteome-scale identification and quantification of isoaspartyl residues in biological samples. *J. Proteome. Res* **2009**, *8*, 4615−4621.

(23) Dai, S. J.; Ni, W. Q.; Patananan, A. N.; Clarke, S. G.; Karger, B. L.; Zhou, Z. S. Integrated proteomic analysis of major isoaspartyl-containing proteins in the urine of wild type and protein L-isoaspartate O-methyltransferase-deficient mice. *Anal. Chem.* **2013**, *85*, 2423−2430.

(24) Geiger, T.; Clarke, S. Deamidation, isomerization, and racemization at asparaginyl and aspartyl residues in peptides. Succinimide-linked reactions that contribute to protein degradation. *J. Biol. Chem.* **1987**, *262*, 785−794.

(25) Li, X. J.; Cournoyer, J. J.; Lin, C.; O'Connor, P. B. Use of O-18 labels to monitor deamidation during protein and peptide sample processing. *J. Am. Soc. Mass. Spectrom* **2008**, *19*, 855−864.

(26) Du, Y.; Wang, F. Q.; May, K.; Xu, W.; Liu, H. C. Determination of deamidation artifacts introduced by sample preparation using O-18-labeling and tandem mass spectrometry analysis. *Anal. Chem.* **2012**, *84*, 6355−6360.

(27) Liu, H. C.; Wang, F. Q.; Xu, W.; May, K.; Richardson, D. Quantitation of asparagine deamidation by isotope labeling and liquid chromatography coupled with mass spectrometry analysis. *Anal. Biochem.* **2013**, *432*, 16−22.

(28) Lyutvinskiy, Y.; Yang, H.; Rutishauser, D.; Zubarev, R. A. In silico instrumental response correction improves precision of label-free proteomics and accuracy of proteomics-based predictive models. *Mol. Cell. Proteomics* **2013**, *12*, 2324−2331.

(29) Nesvizhskii, A. I.; Keller, A.; Kolker, E.; Aebersold, R. A statistical model for identifying proteins by tandem mass spectrometry. *Anal. Chem.* **2003**, *75*, 4646−4658.

(30) Robinson, N. E.; Robinson, A. B. Deamidation of human proteins. *Proc. Natl. Acad. Sci. U.S.A.* **2001**, *98*, 12409−12413.

(31) Wakankar, A. A.; Borchardt, R. T. Formulation considerations for proteins susceptible to asparagine deamidation and aspartate isomerization. *J. Pharm. Sci.* **2006**, *95*, 2321−2336.

(32) Deverman, B. E.; Cook, B. L.; Manson, S. R.; Niederhoff, R. A.; Langer, E. M.; Rosov, I.; Kulans, L. A.; Fu, X.; Weinberg, J. S.; Heinecke, J. W.; Roth, K. A.; Weintraub, S. J. Bcl-xL deamidation is a critical switch in the regulation of the response to DNA damage. *Cell.* **2002**, *111*, 51−62.

(33) Takata, T.; Oxford, J. T.; Demeler, B.; Lampi, K. J. Deamidation destabilizes and triggers aggregation of a lens protein, beta A3-Crystallin. *Protein Sci.* **2008**, *17*, 1565−1575.

(34) Eggleton, P.; Haigh, R.; Winyard, P. G. Consequence of neo-antigenicity of the 'altered self'. *Rheumatology* **2008**, *47*, 567−571.

(35) Johnson, B. A.; Shirokawa, J. M.; Hancock, W. S.; Spellman, M. W.; Basa, L. J.; Aswad, D. W. Formation of isoaspartate at two distinct sites during in vitro aging of human growth hormone. *J. Biol. Chem.* **1989**, *264*, 14262−14271.

(36) Morrison, G. J.; Ganesan, R.; Qin, Z.; Aswad, D. W. Considerations in the identification of endogenous substrates for protein L-isoaspartyl methyltransferase: the case of synuclein. *PLoS One* **2012**, *7*, e43288.

(37) Stephenson, R. C.; Clarke, S. Succinimide formation from aspartyl and asparaginyl peptides as a model for the spontaneous degradation of proteins. *J. Biol. Chem.* **1989**, *264*, 6164−6170.

(38) Cournoyer, J. J.; Lin, C.; Bowman, M. J.; O'Connor, P. B. Quantitating the relative abundance of isoaspartyl residues in deamidated proteins by electron capture dissociation. *J. Am. Soc. Mass. Spectrom* **2007**, *18*, 48−56.

(39) Potter, S. M.; Henzel, W. J.; Aswad, D. W. In vitro aging of calmodulin generates isoaspartate at multiple Asn−Gly and Asp−Gly sites in calcium-binding domains II, III, and IV. *Protein Sci.* **1993**, *2*, 1648−1663.

(40) Daubenberger, C. A.; Tisdale, E. J.; Curcic, M.; Diaz, D.; Silvie, O.; Mazier, D.; Eling, W.; Bohrmann, B.; Matile, H.; Pluschke, G. The N′-terminal domain of glyceraldehyde-3-phosphate dehydrogenase of the apicomplexan Plasmodium falciparum mediates GTPase Rab2-dependent recruitment to membranes. *Biol. Chem.* **2003**, *384*, 1227−1237.

(41) Rivers, J.; McDonald, L.; Edwards, I. J.; Beynon, R. J. Asparagine deamidation and the role of higher order protein structure. *J. Proteome Res.* **2008**, *7*, 921−927.

(42) Filonenko, V. V.; Beresten, S. F.; Rubikaite, B. I.; Kisselev, L. L. Bovine tryptophanyl-tRNA synthetase and glyceraldehyde-3-phosphate dehydrogenase form a complex. *Biochem. Biophys. Res. Commun.* **1989**, *161*, 481−488.

(43) Vegh, M. J.; de Waard, M. C.; van der Pluijm, I.; Ridwan, Y.; Sassen, M. J. M.; van Nierop, P.; van der Schors, R. C.; Li, K. W.; Hoeijmakers, J. H. J.; Smit, A. B.; van Kesteren, R. E. Synaptic proteome changes in a DNA repair deficient Ercc1 mouse model of accelerated aging. *J. Proteome Res.* **2012**, *11*, 1855−1867.

(44) Olalla, L. a.; Gutiérrez, A.; Campos, J. A.; Khan, Z. U.; Alonso, F. J.; Segura, J. A.; Márquez, J.; Aledo, J. C. Nuclear localization of L-type glutaminase in mammalian brain. *J. Biol. Chem.* **2002**, *277*, 38939−38944.

(45) Masson, J.; Darmon, M.; Conjard, A.; Chuhma, N.; Ropert, N.; Thoby-Brisson, M.; Foutz, A. S.; Parrot, S.; Miller, G. M.; Jorisch, R.; Polan, J.; Hamon, M.; Hen, R.; Rayport, S. Mice lacking brain/kidney phosphate-activated glutaminase have impaired glutamatergic synaptic transmission, altered breathing, disorganized goal-directed behavior and die shortly after birth. *J. Neurosci.* **2006**, *26*, 4660−4671.

(46) Makeyev, A. V.; Liebhaber, S. A. The poly(C)-binding proteins: A multiplicity of functions and a search for mechanisms. *RNA* **2002**, *8*, 265−278.

(47) You, F.; Sun, H.; Zhou, X.; Sun, W.; Liang, S.; Zhai, Z.; Jiang, Z. PCBP2 mediates degradation of the adaptor MAVS via the HECT ubiquitin ligase AIP4. *Nat. Immunol* **2009**, *10*, 1300−1308.

(48) Xin, Z.; Han, W.; Zhao, Z.; Xia, Q.; Yin, B.; Yuan, J.; Peng, X. PCBP2 enhances the antiviral activity of IFN-α against HCV by stabilizing the mRNA of STAT1 and STAT2. *PLoS One* **2011**, *6*, e25419.

(49) Ghosh, D.; Srivastava, G. P.; Xu, D.; Schulz, L. C.; Roberts, R. M. A link between SIN1 (MAPKAP1) and poly(rC) binding protein 2 (PCBP2) in counteracting environmental stress. *Proc. Natl. Acad. Sci. U.S.A.* **2008**, *105*, 11673−11678.

(50) Shi, H.; Cordin, O.; Minder, C. M.; Linder, P.; Xu, R. M. Crystal structure of the human ATP-dependent splicing and export factor UAP56. *Proc. Natl. Acad. Sci. U.S.A.* **2004**, *101*, 17628−17633.

(51) Herold, A.; Teixeira, L.; Izaurralde, E. Genome-wide analysis of nuclear mRNA export pathways in Drosophila. *EMBO J.* **2003**, *22*, 2472−2483.

(52) Sahni, A.; Wang, N.; Alexis, J. D. UAP56 is an important regulator of protein synthesis and growth in cardiomyocytes. *Biochem. Biophys. Res. Commun.* **2010**, *393*, 106−110.

(53) Farrar, C. E.; Clarke, S. Diet-dependent survival of protein repair-deficient mice. *J. Nutr. Biochem* **2005**, *16*, 554−561.

(54) Fillenz, M. Physiological release of excitatory amino acids. *Behav. Brain Res.* **1995**, *71*, 51−67.

(55) Daikhin, Y.; Yudkoff, M. Compartmentation of brain glutamate metabolism in neurons and glia. *J. Nutr.* **2000**, *130*, 1026−1031.

(56) Meldrum, B. S. The role of glutamate in epilepsy and other CNS disorders. *Neurology* **1994**, *44*, S14–S23.

(57) Tabatabaie, L.; Klomp, L. W.; Berger, R.; de Koning, T. J. L-Serine synthesis in the central nervous system: a review on serine deficiency disorders. *Mol. Genet. Metab.* **2010**, *99*, 256–262.

(58) Kalhan, S. C.; Hanson, R. W. Resurgence of serine: An often neglected but indispensable amino acid. *J. Biol. Chem.* **2012**, *287*, 19786–19791.

(59) Davis, S. R.; Stacpoole, P. W.; Williamson, J.; Kick, L. S.; Quinlivan, E. P.; Coats, B. S.; Shane, B.; Bailey, L. B.; Gregory, J. F. Tracer-derived total and folate-dependent homocysteine remethylation and synthesis rates in humans indicate that serine is the main one-carbon donor. *Am. J. Physiol. Endocrinol. Metab.* **2004**, *286*, E272–.

Supporting Information

Figure S1. Quantification profiles of protein L-isoaspartyl methyltransferase (PIMT) from both wild type (WT) mice and PIMT-knockout (KO) mice. In total, five peptides were identified by MS/MS as belonging to PIMT. In all WT samples, the PIMT abundance was quantified based on XIC of three or more peptides, while in most KO samples, PIMT was quantified based on only one peptide, ALDVGSGSGILTACFAR. Note that XIC quantification can provide false positives when the m/z and retention times of two peptides overlap within the selected windows. Further analysis using .raw spectra confirmed that, in the PIMT-KO group, there was no MS/MS detection of PIMT at all, which verifies the absence of PIMT enzyme in KO mice.
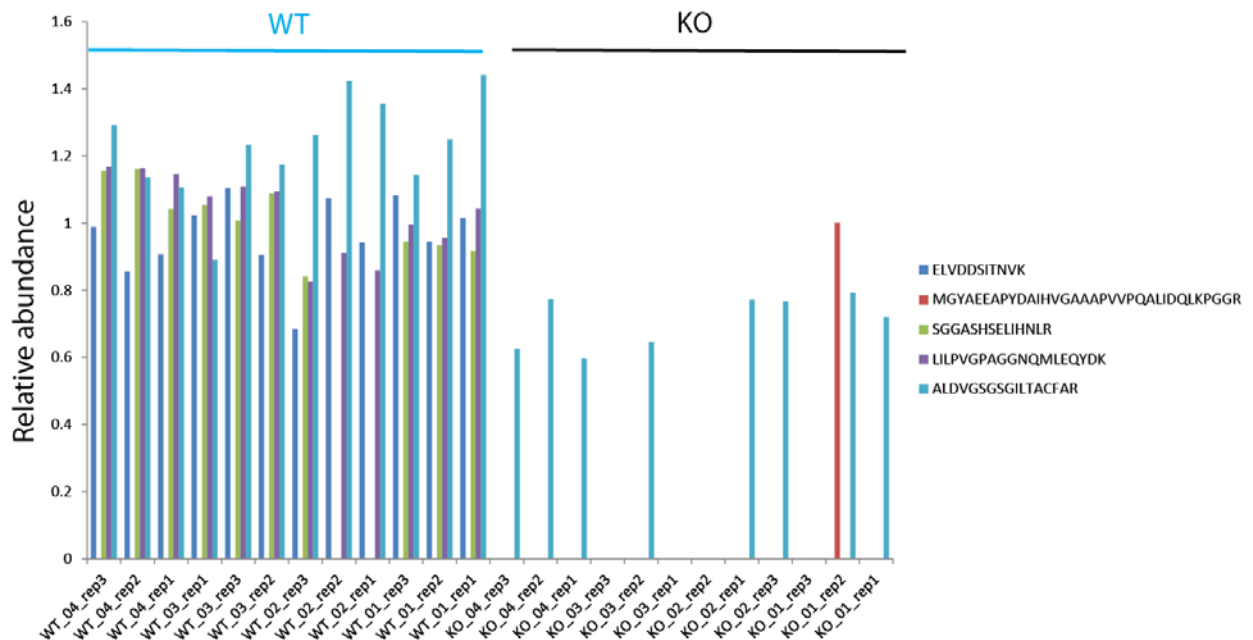
Figure S2. Overall performance of the in-gel digestion method. A: Principal component analysis (PCA) of the quantified protein abundances (SIMCA, $R^2X[cum]=0.508$; $Q^2[cum]=0.014$). KO, PIMT-KO mice; WT, wild-type controls. B: Number of quantified proteins found by both the in-gel digestion method and the FASP method. C: Number of significantly regulated proteins in FASP overlapping with all quantified proteins in the in-gel method; red number indicates the number of proteins with the same regulation direction, while black number - opposite regulation directions.
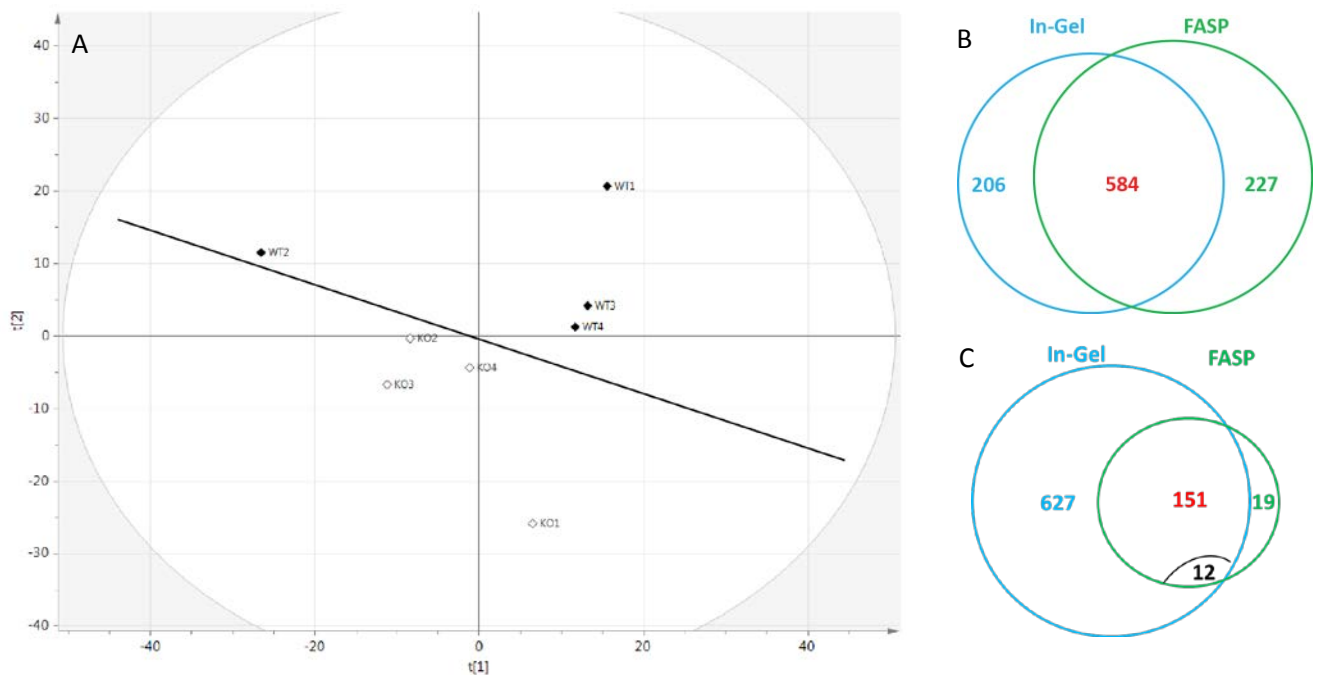
Table S1. *Mouse Information: name, gender, genotype, age, and experimental ID.*

Table S2. *IsoAsp-containing peptide candidates from deamidation of PIMT-KO mice.*

Table S3. *IsoAsp-containing peptide candidates from deamidation of control mice.*

Table S4. *IsoAsp-containing peptide candidates from isomerization of PIMT-KO mice.*

Table S5. *IsoAsp-containing peptide candidates from isomerization of control mice.*

Table S6. *Abundance of isoAsp-containing peptides which were uniquely identified either from WT mice or PIMT-KO mice.*

Table S7. *IsoAsp accumulation ratio of all samples for peptide VFDKDGNGYISAAELR and LVINGKPITIFQER.*

Table S8. *Peptides identified from FASP method.*

Table S9. *Proteins identified from FASP method.*

Table S10. *Proteins quantified from FASP method.*

Table S11. *Proteins significantly regulated comparing wild type control and PIMT-knockout mice by FASP method.*

Table S12. *Peptides identified from in-gel method.*

Table S13. *Proteins identified from in-gel method.*

Table S14. *Proteins quantified from in-gel method.*

Table S15. *Significant regulated proteins that have been supported by both FASP (p < 0.001) and in-gel (same regulation trends as FASP) methods.*

Table S16. *All proteins identified both in FASP and in-gel methods.*

SAMPLE NAME	GENDER	TYPE	AGE	EXP ID
9796	FEMALE	KO	51	KO_01
9802	FEMALE	Control	51	WT_01
9803	FEMALE	KO	51	KO_02
9844	FEMALE	KO	52	KO_03
9845	FEMALE	Control	52	WT_02
9852	FEMALE	KO	52	KO_04
9829	FEMALE	Control	53	WT_03
10308	FEMALE	Control	53	WT_04